A NOVEL HIGH-ISOLATION COMPACT WEARABLE MIMO ANTENNA WITH SEQUENTIAL-ROTATED FEEDING

Xiaolan LIU[1,2,3], Jianxiao LIU[1], Xudong LUO[2]*

*Modern mobile communication equipment requires small size and high integration. Therefore, it is necessary to reduce the mutual coupling between the Multiple Input Multiple Output (MIMO) antenna elements to ensure low correlation between the signals. This paper proposes a novel compact wearable MIMO antenna with a low-profile structure and high isolation, which uses 1mm thick denim as the dielectric substrate. The antenna array realizes high isolation by adopting a sequential rotation technique (SRT) with 2*2 antenna element. The bandwidth of the proposed antenna can effectively cover the band of 2.4GHz for Wireless Local Area Network. The experimental results show that the isolation between antenna elements is greater than 35dB in the required frequency range (1GHz-6GHz), which meets the requirements of wearable MIMO antennas.*

Keywords: MIMO antenna; Wearable; Isolation; Sequential rotation.

1. Introduction

The popularity of intelligent terminals and the vigorous development of mobile services have promoted the rapid development of mobile Internet. In order to meet the requirements of wide band, high capacity, dense sites, reliability and green energy saving, the 5th generation mobile network has entered the commercial stage [1-3]. The Multiple Input Multiple Output (MIMO) technology can significantly improve the data throughput and system reliability without increasing the system bandwidth and transmission power. The MIMO technology has become a research hotspot in academia and industry, being widely used in a variety of mobile communication technology standards. The unique advantages of MIMO technology will become the key technologies of 5g [4].

The MIMO technology has the ability to improve the channel capacity. It can improve the signal-to-noise ratio of communication systems, channel capacity and suppress channel fading [5-6]. The MIMO antenna fully utilizes the multipath transmission at both ends of the transceiver, resulting in large development space. On the premise of unchanged transmission power and spectrum resources, the MIMO antenna can significantly improve the capacity of the communication

[1] Lec., Dept. of Physical and Electronic Information, Hengshui University, China,
[2] Ass., Teachers College for Vocational and Technical Education, Guangxi Normal University, China
[3] Hebei Key Laboratory of Wetland Ecology and Conservation, *luoxudong@gxnu.edu.cn

system and has better reliability [7-9]. For wearable mobile terminals, the antenna distribution space provided by MIMO antennas is extremely limited and these antennas are very harsh, which poses a severe challenge to the decoupling of antenna arrays.

Under the condition of abundant scattering environment, the system capacity of MIMO system depends on the minimum number of antennas at the transmitter and the receiver [10] and increases linearly with the increase in the minimum number. Therefore, increasing the number of antennas at the transmitter and the receiver sides can significantly improve the reliability and effectiveness of MIMO system. Numerous research studies have been conducted on antenna decoupling, including cutting slots on the patch and ground plane [11], branch method of ground plate [12], and decoupling network method [13] and the reverse coupling elimination method commonly used in low profile patch antennas. Tang et al. proposed a dual notch UWB MIMO antenna [14]. By loading decoupling structure on the floor, the whole UWB frequency domain isolation was greater than 15dB. Zhang L G et al. of Xidian University proposed a wearable MIMO antenna, which was a coplanar waveguide antenna [15]. The medium was made of flexible Kapton Polyimide substrate material. Zhu Jianfeng et al. proposed a coupled-fed tri-band MIMO mobile antenna composed of two antenna elements, where each antenna element consisted of a planar inverted-F antenna coupled-fed by a L-shaped driven strip monopole [16]. The bandwidth can be enhanced without increasing the antenna size. In the design of MIMO antenna, the design of multi-antenna elements and their layout are extremely important in order to obtain the required gain, system capacity and various advantages.

This paper applies the sequential rotating technology to the design of wearable MIMO antennas, which reduces the mutual coupling between antenna elements, proposes some new design ideas and programs suitable for MIMO antennas at system terminals, and provides the experimental results.

2. Material and Method

2.1 Sequential Rotation Technique (SRT)

The important factor that determines the diversity performance is the correlation between the diversity branches. When the angular spectrum distribution of the incident wave is fixed, the correlation of the output signal of the antenna can be understood as the degree of the difference after the antenna weights the electromagnetic field of different incident angles. If the incoming wave of different incident angles is independent, the correlation between the output signals of each antenna completely depends on the phase of the antenna center distance and respective pattern.

Let the distance between the two antenna phase centers is *d*. According to the specific situation of the mobile terminal antenna, it is assumed that the phase distribution of the incident field is independent of the incident angle and the polarization of the field, and the phase distribution of the incident field is evenly distributed between degrees.

When multiple antennas are placed adjacent to each other, the electric field of an antenna affect the current distribution of the adjacent antenna, resulting in the radiation pattern distortion of the antenna, and the input impedance changes, which is the mutual coupling effect. Due to the mutual coupling between the antennas, the current on each antenna unit will change, which is different from the current distribution when the antenna is placed in the free space separately. Therefore, pattern, impedance and polarization of the antenna will change, which will have serious impact on the performance and matching of the antenna.

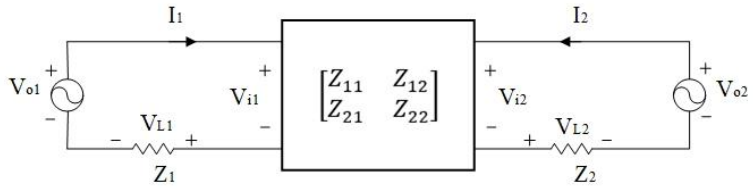

Fig. 1. Equivalent circuit diagram of dual array antenna.

In the design of antenna, the harmful effect of coupling between antenna elements must be considered. The mutual coupling effect between antennas can be described by the coupling matrix. The impedance matrix analysis method uses the circuit model to calculate the mutual impedance between the elements. In order to calculate the coupling matrix, Fig. 1 shows the equivalent circuit diagram of the antenna array comprising of two antennas, which is a typical linear passive two port network. Considering that the antenna array shown in Fig. 1 is at the receiver, V_{i1} and V_{i2} are the induced voltages received from the space, the load impedances are Z_1 and Z_2; the load impedance voltages are V_{L1} and V_{L2}, the currents are I_1 and I_2, and V_{o1} and V_{o2} represent the open circuit voltages.

$$V_o = \begin{bmatrix} V_{o1} \\ V_{o2} \end{bmatrix}, \quad V_L = \begin{bmatrix} V_{L1} \\ V_{L2} \end{bmatrix}, \quad V_i = \begin{bmatrix} V_{i1} \\ V_{i2} \end{bmatrix}, \quad I = \begin{bmatrix} I_1 \\ I_2 \end{bmatrix}, \tag{1}$$

The relationship between voltage and current can be obtained by circuit model analysis,

$$V_o = V_L + V_i \tag{2}$$

$Z = \begin{bmatrix} Z_{11} & Z_{12} \\ Z_{21} & Z_{22} \end{bmatrix}$ represents the mutual coupling impedance matrix, which can be obtained by substituting formula (2),

$$V_L = \begin{bmatrix} V_{L1} \\ V_{L2} \end{bmatrix} = \begin{bmatrix} Z_1 & 0 \\ 0 & Z_2 \end{bmatrix} \begin{bmatrix} I_1 \\ I_2 \end{bmatrix} = \begin{bmatrix} Z_1 & 0 \\ 0 & Z_2 \end{bmatrix} \cdot I \tag{3}$$

$$V_i = \begin{bmatrix} V_{i1} \\ V_{i2} \end{bmatrix} = \begin{bmatrix} Z_{11} & Z_{12} \\ Z_{21} & Z_{22} \end{bmatrix} \begin{bmatrix} I_1 \\ I_2 \end{bmatrix} = Z \cdot I \tag{4}$$

Substituting formulas (3) and (4) into formula (2), the load voltage can be expressed as:

$$V_L = \begin{bmatrix} V_{L1} \\ V_{L2} \end{bmatrix} = \left[I + Z \begin{bmatrix} Z_1 & 0 \\ 0 & Z_2 \end{bmatrix}^{-1} \right]^{-1} \begin{bmatrix} V_{o1} \\ V_{o2} \end{bmatrix} \tag{5}$$

The element $Z_{m(m-1)}$ in the mutual coupling impedance matrix Z represents the mutual coupling impedance between the *m-th* and the *(m-1)st* antennas in the antenna array, which can be written as:

$$Z_{m(m-1)} = R_{m(m-1)} + jX_{m(m-1)} \tag{6}$$

where, $R_{m(m-1)}$ and $X_{m(m-1)}$ represent the mutual impedance and mutual inductance between the *m-th* and the *(m-1)st* antennas, respectively. The magnitude of the mutual coupling impedance is related to the placement of the antenna. When the antenna array is placed flush, $R_{m(m-1)}$ and $X_{m(m-1)}$ can be expressed as [17]:

$$R_{m(m-1)} = \frac{\sqrt{\mu_0}}{4\pi\sqrt{\varepsilon_0}} [2C_i(\mu_0) - C_i(\mu_1) - C_i(\mu_2)] \tag{7}$$

$$X_{m(m-1)} = \frac{\sqrt{\mu_0}}{4\pi\sqrt{\varepsilon_0}} [2S_i(\mu_0) - S_i(\mu_1) - S_i(\mu_2)] \tag{8}$$

In formulas (7) and (8), ε_0 is the dielectric constant, μ_0 is the permeability, *l* is the length of dipole antenna, and *d* is the distance between unit antennas. With the increase of the distance *d*, the mutual impedance and the mutual reactance between the two antennas tend to 0, which shows that when the distance between the two antennas is large enough, the mutual coupling effect between the two antennas will eventually disappear.

The isolation degree describes the degree of mutual independence of the antenna unit ports. The smaller the coupling degree between the antenna units is, the greater the isolation degree will be; and vice versa. For the designed wearable MIMO antenna, the isolation degree is usually greater than 20dB to meet the requirements.

The SRT is a technology that rotates the radiation element and changes the feeding phase in a certain sequence. For sequential rotating array (SRA), there is a certain rotation angle or even orthogonality between adjacent radiating elements, which can reduce the mutual coupling. The traditional microstrip antenna array

rotates in order, assuming that the m radiation elements in the array rotate at an angle of φ_{pm} in the plane, and the phase of the feed point changes by φ_{em} [18]:

$$\varphi_{pm} = (m-1)\frac{p\pi}{nm} \tag{9}$$

$$\varphi_{em} = (m-1)\frac{p\pi}{m} \tag{10}$$

In formulas (9) and (10), p is an integer that represents the number of half turns the element rotates in the plane, m is the total number of elements in the sequential rotated array, n represents the waveform index, and $TM_{11,}$ $n=1$ for microstrip antennas operating with the main mode. Rotating the array antenna in sequence with the unrotated antenna can increase the axial ratio bandwidth and standing wave bandwidth. Hence, such rotation is more conducive to antenna design.

2.2. Antenna Design

Generally, antenna elements are considered to be isotropic and do not interfere with each other. However, in practice, each antenna element is not isotropic and there is mutual coupling between them. Signal processing and code are critically important in MIMO system, and antenna design is the key factor that can fundamentally affect the system implementation. The design of MIMO antenna has the following requirements: reasonable gain, low correlation, multiple diversity, low, and wide lobe. In order to meet these requirements, the spacing of each antenna element, impedance matching, element pattern, mutual coupling among multiple antennas, and element form should be considered while designing the MIMO antenna.

As shown in Fig. 2, the MIMO antenna element includes two semi-circular patches, ground plate and coaxial feed. The size of the antenna dielectric substrate is $w*l*h$, the center coordinates of the left semicircle are (0, 0), and the coordinates of the feeding point are (x_0, y_0).

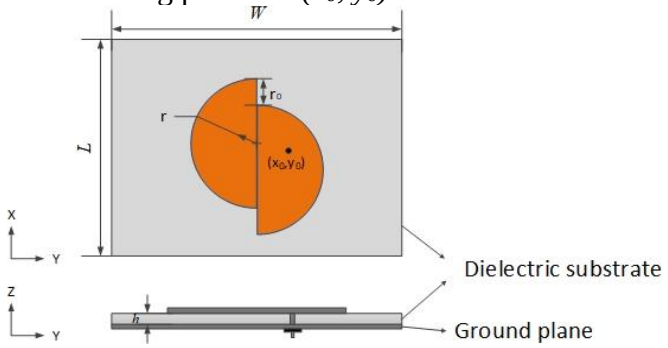

Fig. 2. Geometrical structure of MIMO antenna element.

In this paper, the number of wearable MIMO antenna elements selected is 4, and the indoor environment is rich in multipaths. In order to obtain large spatial diversity gain, the antenna spacing is selected to be about one wavelength and the rotation angle is θ_1-θ_4, as shown in Fig. 3.

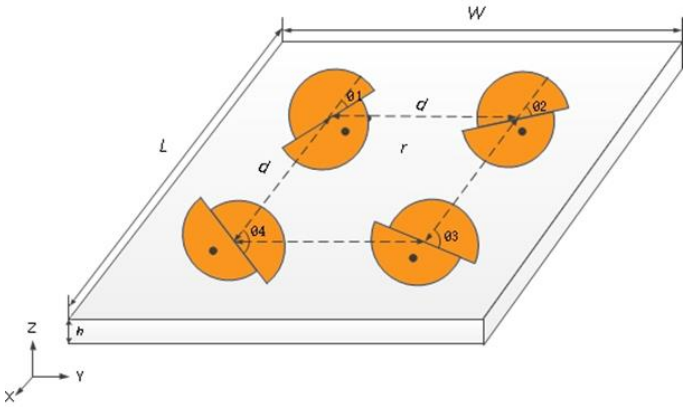

Fig. 3. Geometrical structures of four wearable MIMO antenna elements.

The rotation direction of the four elements is same as the polarization direction of the composed polarization array. Thus, the polarization characteristics of the array can be improved by the dual polarization characteristics, and its axial ratio characteristics are better than that of the ordinary array.

3. Results

When the relative dielectric constant and the thickness h of the dielectric substrate are determined, the resonant frequency value f_c of the circular microstrip antenna is inversely proportional to the radius r of the circular patch, i.e. the resonant frequency decreases with the increase in the radius, and it is not possible to flexibly adjust the distance between the resonant frequencies.

As shown in Fig. 2, the antenna consists of two semi-circular patches, and the resonant frequency is adjusted by changing the radius of each semi-circle patch and the distance between the centers of the two semi-circular patches. When the staggered distance r_0 of the two semicircles does not exceed 0.581 times of patch radius r, with the decrease of radius r, the two resonant frequencies f_{c1} *and* f_{c2} of the antenna gradually shift to high frequency between 1GHz and 6GHz. However, the larger the dielectric constant of the dielectric substrate, the higher the two resonant frequencies shift to low frequencies at the same time. The thickness h of the dielectric substrate mainly affects the bandwidth of the antenna. The bandwidth increases to -10dB with the increase in the thickness of the dielectric substrate. The two resonant frequencies of the antenna are 2.45GHz and 3.5GHz, and the values of r and r_0 are obtained. Simulation and optimization are

conducted and the antenna size parameters are obtained as shown in Table 1.

Table 1

Partial Parameters of Antenna Element

Parameters	W	L	h	r	r_0	x_0	y_0
Value	100	100	1	23	5	0	10

Fig. 4 shows the physical model of the antenna processed using the parameters listed in Table 1. The antenna metal patch is pasted on ordinary denim cloth with a relative dielectric constant of 1.511, a dielectric loss tangent of 0.018, a thickness of 1mm, and a feeding position of (0, 10). The connector used is SMA adapter. All tests were carried out in the anechoic chamber, and the vector network analyzer used in the test was Agilent e5071c.

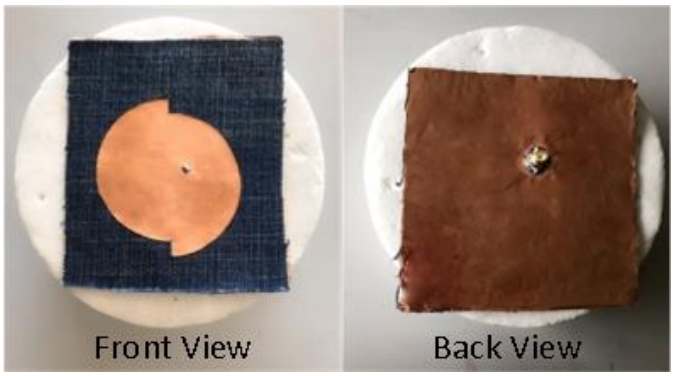

(a) (b)

Fig. 4. Photograph of wearable MIMO antenna element (a) front view (b) back view.

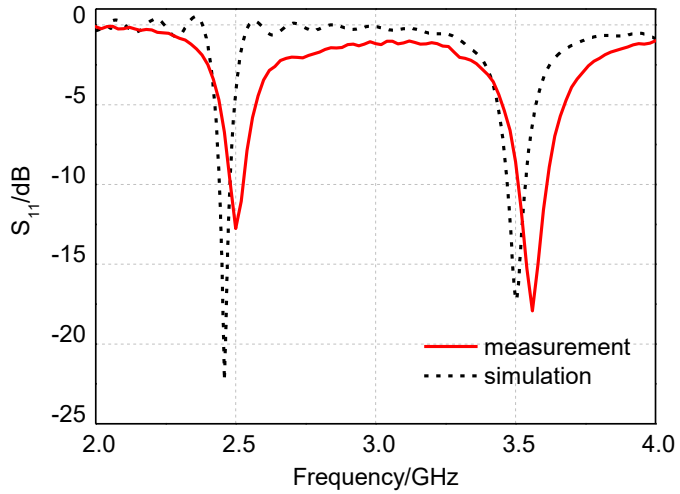

Fig. 5. Comparison of measured and simulated $|S_{11}|$ of MIMO antenna element.

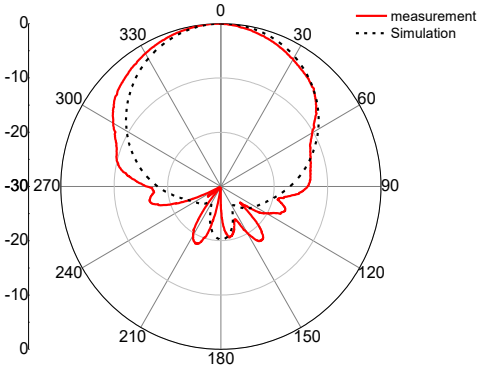
measurement
Simulation
0
30
60
90
120
150
180
210
240
270
300
330
0
-10
-20
-30
-20
-10
0

(a)

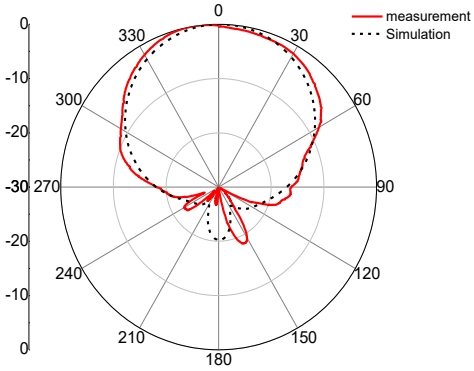
measurement
Simulation
0
30
60
90
120
150
180
210
240
270
300
330
0
-10
-20
-30
-20
-10
0

(b)

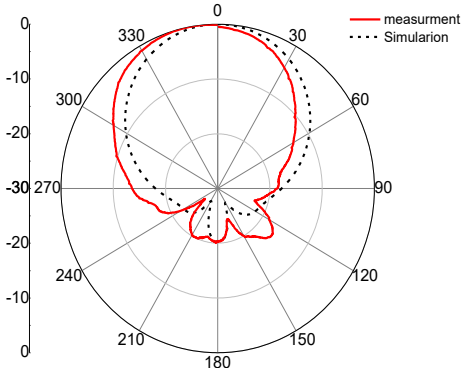
measurment
Simularion
0
30
60
90
120
150
180
210
240
270
300
330
0
-10
-20
-30
-20
-10
0

(c)

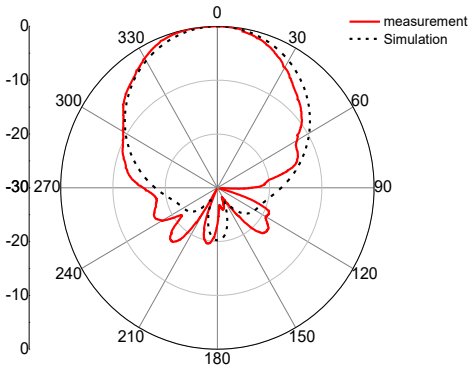

(d)

Fig. 6. Comparison of directivity diagrams of wearable MIMO antenna element at each frequency point (a) 2.45 GHz-E plane (b) 2.45 GHz-H plane (c) 3.5 GHz-E plane (d) 3.5 GHz-H plane

The physical test and the simulation results of the antenna element are similar to those of Figs. 5 and 6. Due to the existence of the metal ground plate, the backward radiation of the antenna is small, which meets the requirements of wearable antenna. As shown in Fig. 7, the antenna is attached to a plastic cylinder with a diameter of 70mm (the average diameter of a human arm) for bending performance test. Figs. 8 and 9 show the comparison of the reflection coefficient curve and the main polarization pattern of the antenna element in bending and flat states, respectively.

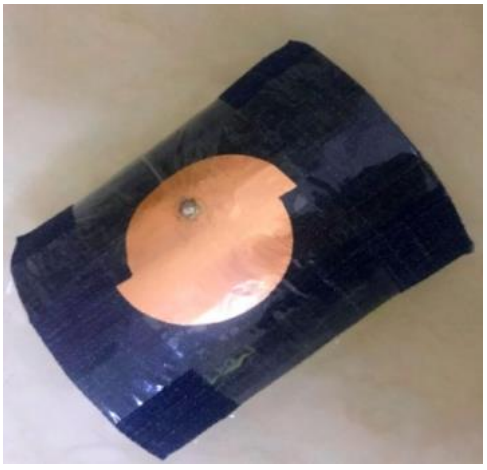

Fig. 7. Photograph of antenna element physical model.

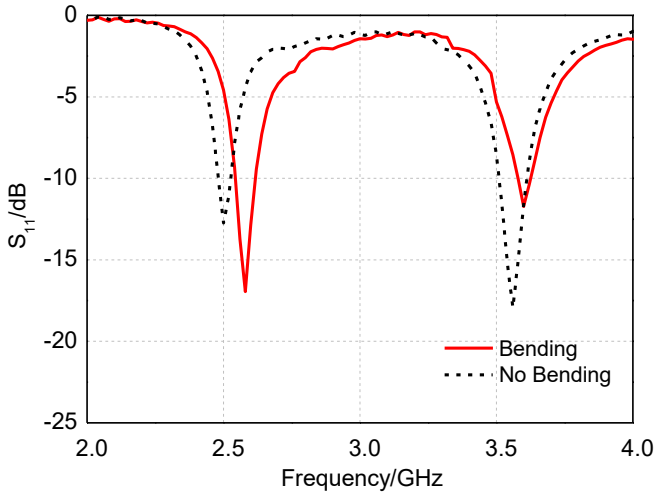

Fig. 8. Comparison of $|S_{11}|$ of antenna element in bending and flat states.

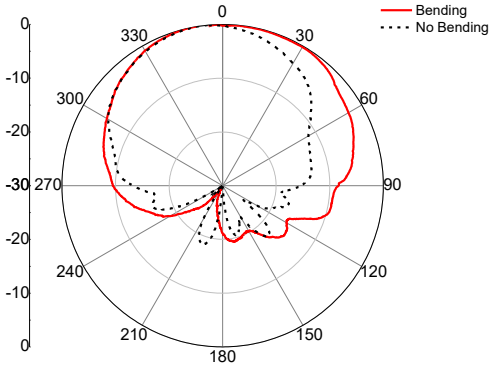

(a)

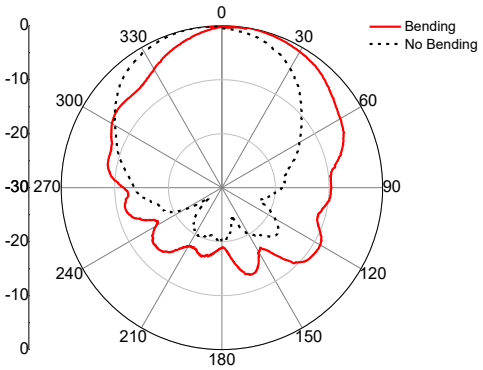

(b)

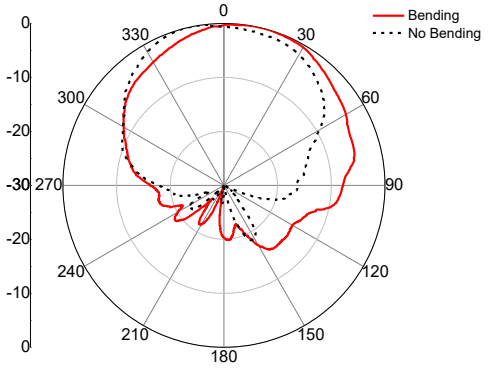

(c)

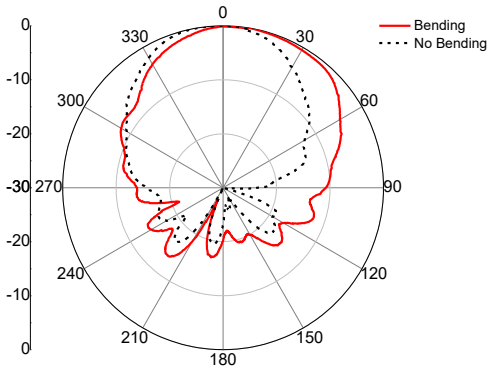

(d)

Fig. 9. Measured patterns of circular antenna in bending and flat states at each frequency point (a) 2.45 GHz-E plane (b) 2.45 GHz-H plane (c) 3.5 GHz-E plane (d) 3.5 GHz-H plane.

As can be seen from Fig. 8, the resonant frequency of the antenna in the curved state is shifted to a high frequency compared with that in the flat state. However, it can be seen from Fig. 9 that the front-back ratio of the pattern increases after the antenna is bent, which is due to the radiation of surface waves excited by the edge of the antenna due to the bending of the antenna.

Multi-antenna layout is the application of antenna diversity technology. It adopts a reasonable layout mode in the antenna distribution space to obtain various antenna diversity gains. As shown in Fig. 3, the four antenna elements are rotated by θ_1- θ_4 in the same direction as the polarization direction, and the antenna element spacing is *d*. The parameters of wearable MIMO antenna are listed in Table 2, and the simulation results are shown in Fig. 10.

Table 2

Partial Parameters of Wearable MIMO Antenna.

Parameters	W	L	h	r	r_0	d	θ_1	θ_2	θ_3	θ_4
Value(mm)	150	150	1	23	2	40	0°	45°	90°	135°

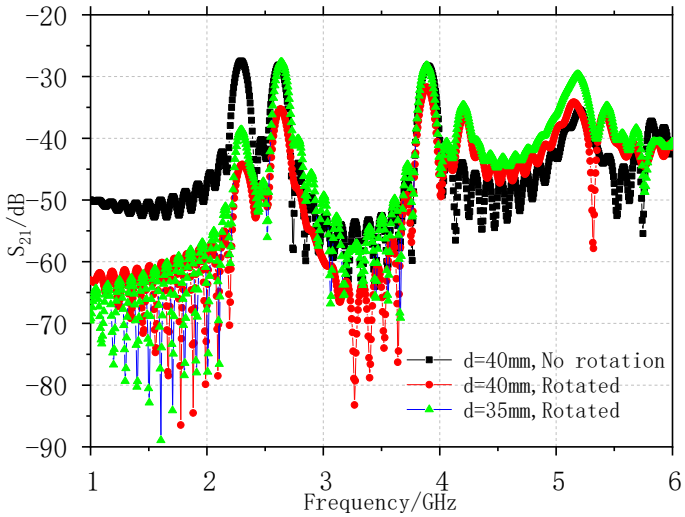

(a)

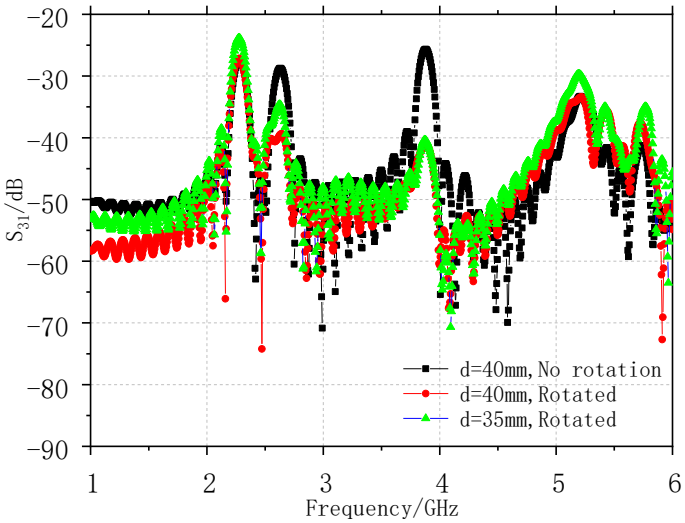

(b)

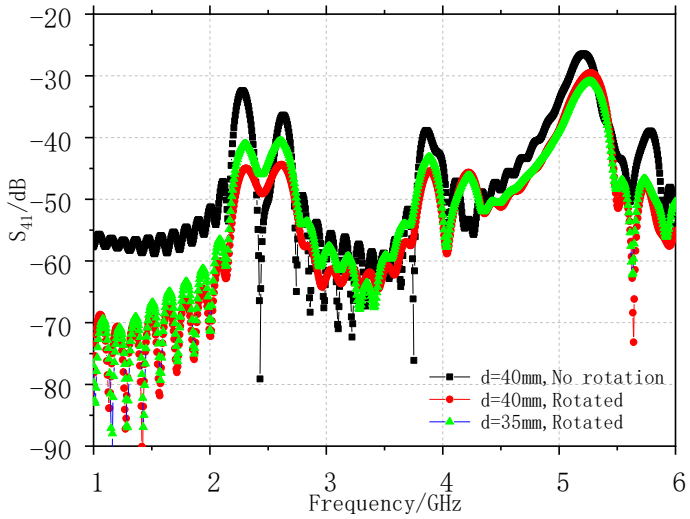
−20
−30
−40
−50
−60
−70
−80
−90
S41/dB
1
2
3
4
5
6
Frequency/GHz
d=40mm, No rotation
d=40mm, Rotated
d=35mm, Rotated

(c)

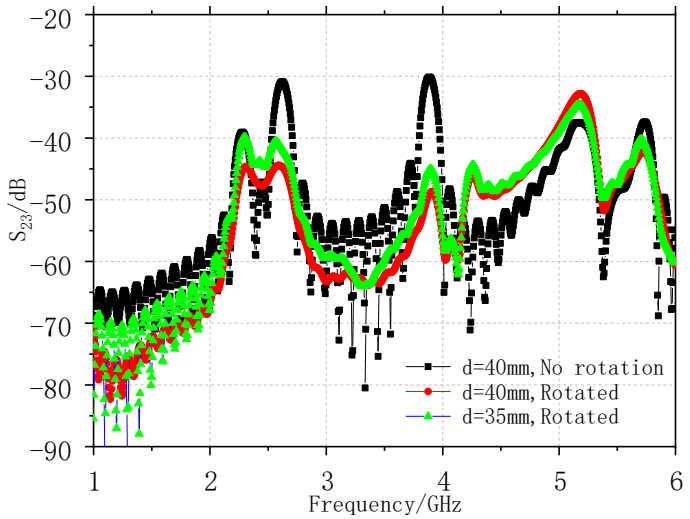
−20
−30
−40
−50
−60
−70
−80
−90
S23/dB
1
2
3
4
5
6
Frequency/GHz
d=40mm, No rotation
d=40mm, Rotated
d=35mm, Rotated

(d)

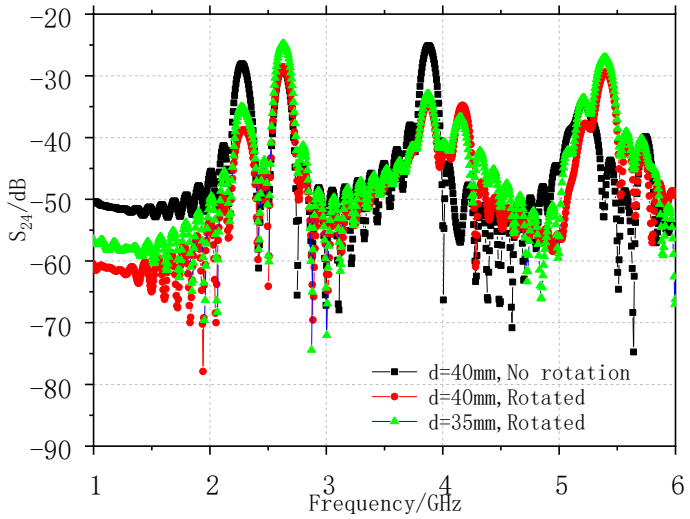

(e)

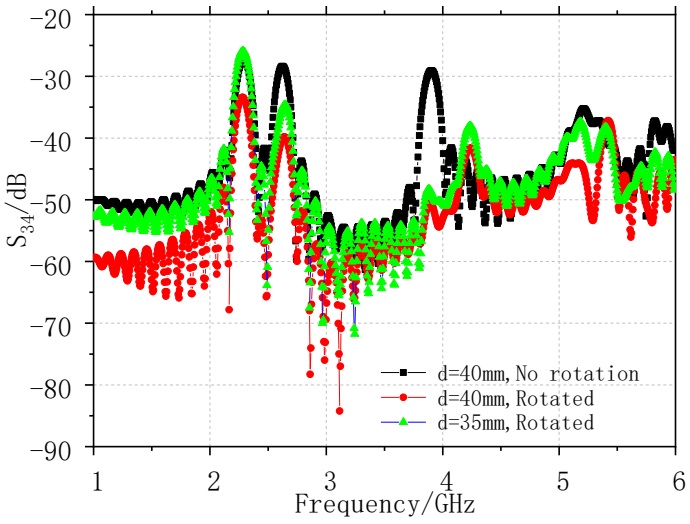

(f)

Fig. 10. Simulation results of wearable MIMO antenna element isolation (a) S21 (b) S31 (c) S41 (d) S23 (e) S24 and (f) S34.

It can be seen from the simulation results that the isolation between antenna elements is improved by using the sequential rotating feed technology. At the same time, the larger the spacing of each antenna element, the higher the isolation of MIMO antenna system, reaching more than 25dB. Fig. 11 shows the

image of the physical antenna made according to the size parameters listed in Table 2. The medium is made of 1mm thick denim cloth, with a relative dielectric constant of 1.511 and a dielectric loss tangent of 0.018. The antenna and the ground plane are both made of cut copper foil tape.

Fig. 11. Photo of sequentially rotating wearable MIMO antenna.

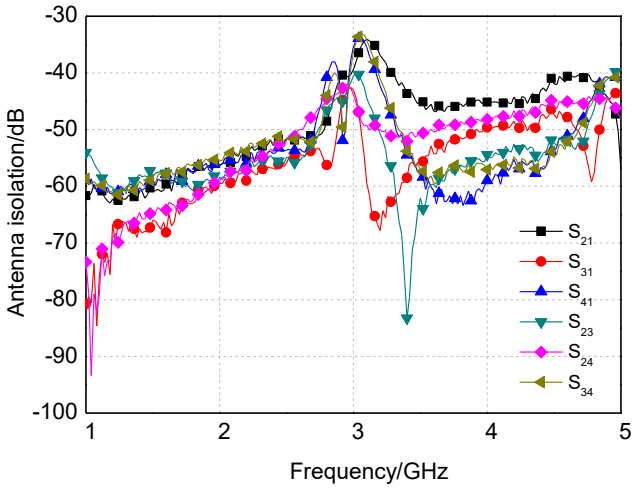

Fig. 12. Measured results of the wearable MIMO antenna.

Table 3

Isolation between Antenna Elements

Isolation	$\|S_{21}\|$	$\|S_{31}\|$	$\|S_{41}\|$	$\|S_{23}\|$	$\|S_{24}\|$	$\|S_{34}\|$
Value(dB)	-35	-39	-35	-39	-42	-36

From Fig. 12, the isolation between each antenna element is obtained and is listed in Table 3. In this section, the sequential rotating feed technology is

applied to MIMO system. It can be seen that the isolation between each antenna element in the required frequency band is greater than 35dB.

4. Discussion

The reasons for the error are mainly as follows. Firstly, the shape and the size of the antenna patch cut by hand are deviated, resulting in the radius change of the circular patch and the change of resonant frequency in the measurement results. Secondly, the thickness of denim cloth can easily change after being pasted with metal floors and metal patches, resulting in bandwidth changes. The errors caused by manual welding of SMA adapters should also be considered.

Due to the mutual coupling between antennas, the current on each antenna element changes, which is different from the current distribution when it is placed in the free space separately. Thus, the pattern, the impedance and the polarization of the antenna change, which seriously impact the performance and matching of the antenna. In the design of antenna, the negative effect of coupling between the antenna elements should be considered. In 2018，Kayabasi et al. proposed a quad-port multi-polarized ultra-wideband MIMO antenna system [19] consisting of four triangular monopole elements and neutralization ring structures. The monopoles were back-to-back positioned in symmetrical and orthogonal arrangement, and they radiated towards four directions without interference. Thus, the diversity performance was improved. Banothu et al. placed the SRR element in between two element MIMO antenna for isolating the mutual coupling effect [20]. In 2019, Hasan et al. proposed monopole antenna consisting of a defected ground structure with two slits and a notch placed at optimum positions to increase the isolation [21].

5. Conclusion

The MIMO technology can improve the system throughput and link stability of wireless communication system. Under ideal conditions, the channel capacity of MIMO system increases linearly with the increase in the number of antennas. However, the spatial correlation, the scattering environment around the antenna and the mutual coupling effect of the antenna all affect the performance of the MIMO system. Especially, when the distance between the antenna elements in the antenna array is not appropriate, there will be strong mutual coupling effect. The influence of mutual coupling effect on the MIMO system cannot be ignored. This paper firstly introduces the calculation method of the coupling matrix.

Compared with the conventional antenna array, the sequential rotating array can significantly increase the axis ratio and standing wave bandwidth of the array and is more conducive to the design of the antenna. This paper proposes a 2*2 wearable MIMO antenna that uses sequential rotating feed technology to increase the isolation between each antenna element. The isolation between the elements in the required frequency band is greater than 35dB. The experimental results demonstrate that the proposed antenna has high radiation efficiency, small backward radiation and good performance, which make the proposed antenna suitable for wearable system applications.

Acknowledgments

This work has been fully supported by the scientific research project of Hengshui University (No. 2018GC16) and Hebei Key Laboratory of Wetland Ecology and Conservation (No. hklz201906).

REFERENCES

[1]. *L. Hairui, Y. Junsheng, H. Peter, et al,* "A Multichannel THz Detector Using Integrated Bow-Tie Antennas", International Journal of Antennas and Propagation, **vol. 2**, no. 1, 2013, pp. 1-8.

[2]. *D. Feng, C. Jiang, G. Lim, et al,* "A survey of energy-efficient wireless communications", IEEE Communications Surveys & Tutorials, **vol. 15**, no. 1, 2013, pp. 167-178.

[3]. *Z. Hasan, H. Boostanimehr, V. K. Bhargava,* "Green Cellular Networks: A Survey, Some Research Issues and Challenges", IEEE, 2011, pp. 524-540.

[4]. *A. Lozano, R. W. Heath, J. G. Andrews,* "Fundamental Limits of Cooperation", IEEE Transactions on Information Theory, **vol. 59**, no. 9, 2013, pp. 5213-5226.

[5]. *H. Ren, N. Liu, C. Pan, et al,* "Energy Efficiency Optimization for MIMO Distributed Antenna Systems", **vol. 66**, no. 3, 2017, pp. 3276-2288.

[6]. *A. Toktas,* "G-shaped band-notched ultra-wideband MIMO antenna system for mobile terminals", Iet Microwaves Antennas & Propagation, **vol. 11**, no. 5, 2017, pp. 718-725.

[7]. *S. Jehangir, S. Sharawi, Atif Shamim,* "A Highly Miniaturized Semi-Loop Meandered Dual-band MIMO Antenna System", Iet Microwaves Antennas & Propagation, **vol. 12**, no. 6, 2018, pp. 864-871.

[8]. *A. Thakur, A. Kumar, N. Gupta, et al,* "Secrecy Outage Performance Analysis of MIMO Underlay Cognitive Radio Networks with Delayed CSI and Transmitter Antenna Selection", International Journal of Communication Systems, **vol. 5**, no.1, 2019, pp. 1-12.

[9]. *Elwi, A. Taha,* "A Miniaturized Folded Antenna Array for MIMO Applications", Wireless Personal Communications, **vol. 9**, no.1, 2017, pp. 1-13.

[10]. *W. H. Ni, X. D. Dong,* "Hybrid Block Diagonalization for Massive Multiuser MIMO Systems", IEEE Transactions on Communications, **vol. 64**, no.1, 2015, pp. 201-211.

[11]. *A. Ghalib, M. S. Sharawi,* "TCM Analysis of Defected Ground Structures for MIMO Antenna Designs in Mobile Terminals", IEEE Access, **vol. 99**, no.1, 2017, pp. 1-1.

[12]. *S. R. Thummaluru, R. Kumar, R. K. Chaudhary,* "Isolation Enhancement and Radar Cross Section Reduction of MIMO Antenna With Frequency Selective Surface", IEEE Transactions on Antennas & Propagation, 2018, PP. 1-1.

[13]. *C. J. Malathi, D. Thiripurasundari,* "Bandwidth Enhanced MIMO antenna for LTE bands using Split Ring Resonators and Stubs", Advanced Electromagnetics, **vol. 7**, no.2, 2018, pp. 36-40.

[14]. *T. C. Tang, K. H. Lin,* "An ultrawideband mimo antenna with dual band-notched function", IEEE Antennas and Wireless Propagation Letters, **vol. 13**, no.1, 2014, pp. 1076-1079.

[15] *Z. Lin Guang, W. Hui Xia, L. Hao,* "Wearable MIMO Antennas Using Characteristic Mode", Journal of Microwaves, **vol. 8**, no.1, 2016, pp. 470-473.

[16]. *J. Zhu, B. Feng, L. Deng, et al,* "Coupled-fed tri-band MIMO mobile antenna for WWAN and LTE applications", Microwave and Optical Technology Letters, **vol. 59**, no.2, 2017, pp. 463-468.

[17]. *C. A. Balanis,* Antenna Theory: Analysis and Design. Hoboken: John Wiley and Sons, Inc., 2005, pp. 471-479.

[18]. *I. J. Chen, C. S. Huang, P. Hsu,* "Circulary polarized patch antenna array fed by coplanar waveguide", IEEE Trans, **vol. 52**, no.6, 2004, pp. 1607-1609.

[19]. *A. Kayabasi, A. Toktas, E. Yigit, et al,* "Triangular quad-port multi-polarized UWB MIMO antenna with enhanced isolation using neutralization ring", AEU-International Journal of Electronics and Communications, **vol. 85**, no.1, 2018, pp. 47-53.

[20]. *Y. V. N. R. S. Banothu, P. Siddaiah,* "Designing a compact MIMO antenna by inserting SRR element to improve the performance", 2018 Conference on Signal Processing And Communication Engineering Systems (SPACES). IEEE, 2018.

[21]. *M. N. Hasan, S. Chu, S,* "Bashir A DGS monopole antenna loaded with U ： hape stub for UWB MIMO applications", Microwave and Optical Technology Letters, 2019.